

# Nanohybridization of Polyoxometalate Clusters and Single-Wall Carbon Nanotubes: Applications in Molecular Cluster Batteries\*\*

Naoya Kawasaki, Heng Wang, Ryo Nakanishi, Shun Hamanaka, Ryo Kitaura, Hisanori Shinohara, Toshihiko Yokoyama, Hirofumi Yoshikawa,\* and Kunio Awaga\*

Single-wall carbon nanotubes (SWNTs) are promising materials for nanoelectronics owing to their unique properties, including their large surface areas, specific electrical conductivity, excellent gas-adsorption characteristics, and significant mechanical strength.<sup>[1]</sup> In fact, as the best and most available one-dimensional nanomaterials, they have wide applications in materials science,<sup>[2]</sup> sensor technology,<sup>[3]</sup> catalysis<sup>[4]</sup> and biomedical fields.<sup>[5]</sup> They are also applicable to nanostructured electrodes to realize high-performance rechargeable batteries<sup>[6]</sup> and super-capacitors,<sup>[7]</sup> as they can provide fast transport pathways for both electrons and lithium ions.

We have recently proposed molecular cluster batteries (MCBs)<sup>[8]</sup> that consist of a lithium anode and cathode-active material based on polynuclear metal complexes (molecular clusters) to achieve both high battery capacity and fast charging/discharging. We prepared an MCB of Mn12 ( $\text{Mn}_{12}\text{O}_{12}(\text{CH}_3\text{COO})_{16}(\text{H}_2\text{O})_4$ ), which is well known as a single-molecule magnet,<sup>[9]</sup> because this molecule undergoes a multi-electron redox reaction.<sup>[10]</sup> Mn12-MCBs can possess an extremely high capacity over  $200 \text{ Ah kg}^{-1}$ , which is larger than that of the lithium ion batteries, owing to a multi-electron redox process between  $\text{Mn}^{2+}$  and  $\text{Mn}^{3+}$ .<sup>[11]</sup> We have previously shown that the molecular clusters are promising cathode-active materials, but their most important feature has not yet been utilized. More specifically, as we made the cathodes by mixing microcrystals of the molecular clusters and vapor-grown carbon fibers (VGCF) with a binder

(Supporting Information, Figure S1), there was no nanoscale dispersion of the cluster molecules, so that the battery reaction was associated with frictional penetration/removal of lithium ions into/from the microcrystals and with non-smooth electron transfer between the cluster molecules and the electrode. These drawbacks brought about problems such as a slow charging/discharging rate and insufficient cyclability.

Herein, we examine nanohybridization between a well-known molecular cluster, namely a polyoxometalate (POM), and SWNTs, to achieve both smooth electron transfer through SWNTs and quick lithium-ion diffusion (Figure 1).

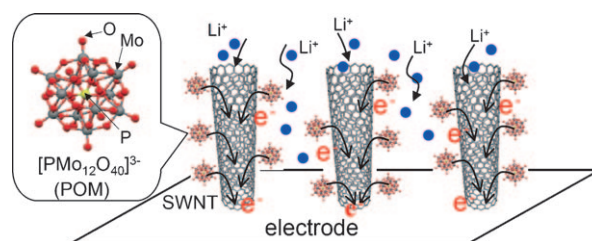


**Figure 1.** Expected battery reactions in the POM/SWNT hybrid materials.

POMs exhibit a rich diversity of properties such as luminescence, catalysis, and magnetism.<sup>[12]</sup> Their reversible multi-electron redox behavior has also been utilized for rechargeable batteries; some of POMs, such as  $[\text{PMo}_{12}\text{O}_{40}]^{3-}$  and  $[\text{PW}_{12}\text{O}_{40}]^{3-}$ ,<sup>[13]</sup> can be cathode-active materials of lithium batteries with large capacities. Although POM-integrated SWNTs have been prepared for spintronics<sup>[14]</sup> and catalysis,<sup>[15]</sup> there has been no report of their applications to battery cathodes. We will present herein the selective adsorption of POMs on SWNTs and the battery performance of this POM/SWNT hybrid material.

A representative Keggin-type POM,  $\text{TBA}_3[\text{PMo}_{12}\text{O}_{40}]$  ( $\text{TBA} = [\text{N}(\text{CH}_2\text{CH}_2\text{CH}_2\text{CH}_3)_4]^+$ ; see Figure 1), was prepared according to the literature method.<sup>[16]</sup> SWNTs were purchased from UNIDYM and were purified using a procedure reported by Nakashima et al.<sup>[17]</sup> (Supporting Information, Figure S2). To graft the POM molecules onto the surface of SWNTs, an acetonitrile solution (5 mL) of  $\text{TBA}_3[\text{PMo}_{12}\text{O}_{40}]$  (40 mg, 16 mmol) was added to a toluene suspension (50 mL) of the purified SWNTs (80 mg) under vigorous stirring at room temperature.<sup>[18]</sup> After stirring until the turbidity of the solution disappeared, the solution was filtered using a membrane filter with a pore diameter of  $0.1 \mu\text{m}$ . Finally, the precipitation was washed with toluene and dried under

[\*] N. Kawasaki, H. Wang, R. Nakanishi, S. Hamanaka, Dr. R. Kitaura, Prof. H. Shinohara, Dr. H. Yoshikawa, Prof. K. Awaga  
Department of Chemistry and  
Research Centre for Materials Science, Nagoya University  
Furo-cho, Chikusa, 464-8602 Nagoya (Japan)  
Fax: (+81) 52-789-2484  
E-mail: yoshikawah@mbox.chem.nagoya-u.ac.jp  
awaga@mbox.chem.nagoya-u.ac.jp

Prof. K. Awaga  
CREST, JST  
Furo-cho, Chikusa, 464-8602 Nagoya (Japan)  
Prof. T. Yokoyama  
Institute for Molecular Sciences  
444-8585 Okazaki (Japan)

[\*\*] This work has been performed with the approval of PF PAC (Proposal Nos 2008G586, 2009G528, and 2010G557). The authors are grateful to the Ministry of Education, Culture, Sports, Science, and Technology (MEXT) of Japan for a Grant-in-Aid for Scientific Research.

Supporting information for this article is available on the WWW under <http://dx.doi.org/10.1002/anie.201007264>.

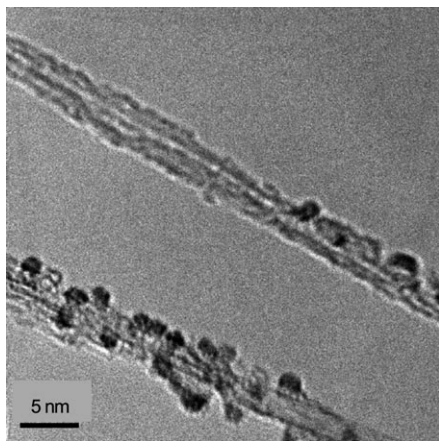


**Figure 2.** TEM image of the POM/SWNT hybrid material.

vacuum. The POM concentration in this POM/SWNT hybrid material was about 30 wt %.

Figure 2 shows a transmission electron microscopy (TEM) image of the POM/SWNT hybrid. The SWNT bundles are decorated by dark spots with a diameter of about 1.5 nm, which corresponds to the molecular size of  $[\text{PMo}_{12}\text{O}_{40}]^{3-}$ . It is considered that the individual POM molecules are separately grafted onto the surfaces of the SWNTs. A low-magnification TEM image (Supporting Information, Figure S3) also supports this feature. Figure 3a depicts the energy-dispersive X-ray (EDX) spectrum for the TEM image area shown in Figure 2. It confirms the presence of molybdenum and also carbon; the peaks for copper are ascribed to TEM grids. The

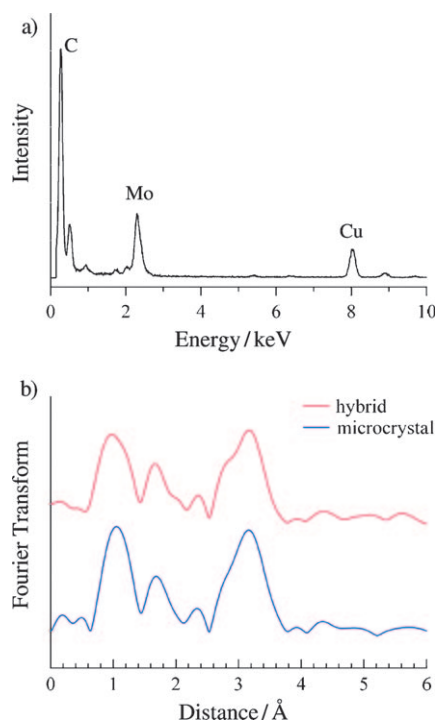


**Figure 3.** a) EDX and b) Mo K-edge EXAFS spectra of the POM/SWNT hybrid material.

surface coverage of the POM molecules on the SWNTs is estimated to be 10 % from the TEM images, assuming that the contact area of one POM molecule is 1.5 nm<sup>2</sup> and the surface area of SWNT is 4.4 nm<sup>2</sup> per unit length (1 nm). It is notable that the surfaces of the SWNTs appear to be rough compared with those of the purified pristine SWNTs (Supporting Information, Figure S2). This difference is probably caused by the tetrabutylammonium cations adsorbed onto the surfaces, as it is known that organic cations coat SWNTs.<sup>[15]</sup> It is speculated that the anionic  $[\text{PMo}_{12}\text{O}_{40}]^{3-}$  ion is electrostatically attracted by the organic cations on SWNTs.

Mo K-edge XAFS analyses were performed on both authentic  $\text{TBA}_3[\text{PMo}_{12}\text{O}_{40}]$  and the POM/SWNT hybrid material to examine the structure of  $[\text{PMo}_{12}\text{O}_{40}]^{3-}$  after nanohybridization. Fourier transforms of the  $k^3\chi(k)$  functions for the two samples (the  $k$  range is 3.5–13.0 Å<sup>−1</sup>) are compared in Figure 3b.  $\text{TBA}_3[\text{PMo}_{12}\text{O}_{40}]$  exhibits four main peaks at 1.0, 1.8, 2.3, and 3.1 Å; the first three peaks are assignable to the Mo–O distances and the last to Mo–Mo. The curvature and peak positions of the hybrid material completely agree with those for  $\text{TBA}_3[\text{PMo}_{12}\text{O}_{40}]$ , indicating that  $[\text{PMo}_{12}\text{O}_{40}]^{3-}$  on the surface of SWNTs suffers from little structural change.

The resonant Raman spectra were measured on the purified SWNTs and the POM/SWNT hybrid at an excitation wavelength of 514 nm (Supporting Information, Figure S4). These two samples exhibit three bands, assigned to the radial breathing mode (RBM) at 200–230 cm<sup>−1</sup>, the defect mode (D) at 1344 cm<sup>−1</sup>, and the longitudinal and transverse modes (G) at 1590 cm<sup>−1</sup>. The intensity ratio of the D and G modes, which is known to reflect the degree of surface defects on SWNTs, is 4.75 or 6.21 for SWNT or POM/SWNT, respectively. This small difference between the two values means that the nanohybridization does not bring about a significant increase of surface defects in SWNTs. A cyclic voltammogram of the POM/SWNT material is depicted in the Supporting Information, Figure S5. This figure shows a broad redox wave, which is typical of solid-state redox active materials, and indicates a multielectron reaction of the POMs on SWNTs.

We examined the battery performance of the POM/SWNT hybrid material as a cathode-active material for MCBs. The cathode was made by mixing POM/SWNT, carbon black, and polyvinylidene fluoride (PVDF) at a weight ratio of 30:50:20, and a lithium foil was used as the anode. The electrolyte was a 1M  $\text{LiPF}_6$  solution of 1:1 v/v ethylene carbonate (EC)/diethyl carbonate (DEC). The battery coin cells were fabricated in an inert atmosphere. For a control experiment, we also prepared the coin cells using POM microcrystals; the cathode (Supporting Information, Figure S6) was fabricated by mixing POM microcrystals, carbon black, and PVDF. In these cathode fabrications, the POM concentration was regulated to be 10 wt %. The charging/discharging measurements were carried out in the voltage range of 1.5–4.2 V on a Hokuto HJ1001-SM8A, and the specific charging/discharging capacities were calculated based on the weight of  $\text{TBA}_3[\text{PMo}_{12}\text{O}_{40}]$  in the cathode.

Figure 4a shows the first charging/discharging curves for the POM/SWNT (solid line) and microcrystalline POM (broken line) batteries, obtained with a constant load current

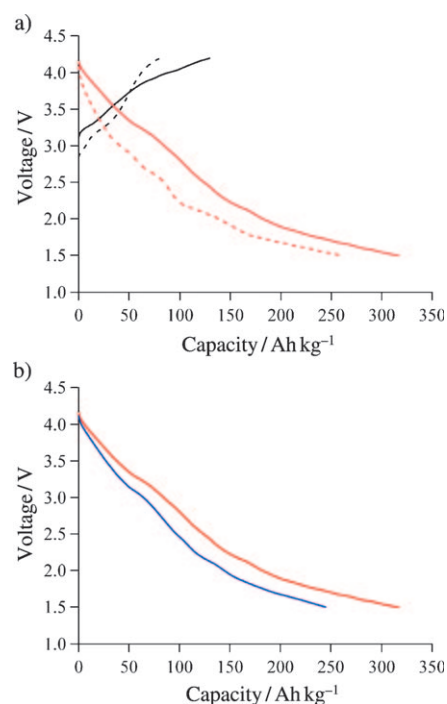


**Figure 4.** a) First charging (black) and discharging (red) curves of the MCBs based on the POM/SWNT hybrid material (—) and the POM microcrystals (----). b) First discharging curves of the POM/SWNT hybrid material with load currents of 1 mA (red) and 2 mA (blue).

of  $I=1.0$  mA. In the first charging processes of the two batteries (black curves), the voltage quickly increases from the initial value (ca. 3.0 V) to 4.2 V. It is likely that these pristine batteries are nearly in the charged states. The first discharging of the microcrystalline POM battery (red, broken curve) indicates a gradual voltage decrease and a high battery capacity of ca. 260 Ah kg<sup>-1</sup> at 1.5 V. This value, which is similar to the one reported previously for POMs,<sup>[13]</sup> can be explained by assuming a redox change between Mo<sup>6+</sup> and Mo<sup>4+</sup> on the 12 molybdenum ions in the POM. The first discharging curve for the POM/SWNT hybrid MCB (red, solid) shows a similar behavior, but the capacity reaches about 320 Ah kg<sup>-1</sup>, which is larger than that of the microcrystal-POM MCB by 60 Ah kg<sup>-1</sup>. To confirm the effect of nanohybridization, we fabricated a cathode by mixing microcrystals of POM, SWNTs carbon black, and PVDF without nanohybridization between POMs and SWNTs and examined its battery performance. The obtained battery capacity was very similar to that of the microcrystalline POM MCB (Figure S7), thus indicating that the excess capacity of the POM/SWNT hybrid battery cannot be explained by an electron storage effect of SWNTs. The large capacity of the POM/SWNT battery suggests a further reduction of the POMs in it.

The cycle performance, as determined from the first ten charging/discharging processes, is given in the Supporting Information, Figure S8. There is no significant decrease in capacity for either the POM/SWNT or the microcrystalline POM MCBs, indicating that POMs are very stable under the solid-state electrochemical redox changes.

Figure 4b shows the first discharging curves of the POM/SWNT MCBs with load currents of  $I=1.0$  and 2.0 mA. With this increase in load current, the voltage drop is enhanced, but the curve of  $I=2.0$  mA still indicates a battery capacity of 250 Ah kg<sup>-1</sup> at 1.5 V, which is similar to that of the microcrystalline POM MCBs obtained with  $I=1.0$  mA. These results indicate that the nanohybridization enables the charging/discharging rate to be twice as large as that of the microcrystalline POM MCBs. This difference is probably caused by the nanohybrid structure bringing about smooth electron transfer and lithium ion diffusion.

In summary, we have developed a nanohybrid system between the POM clusters and the SWNTs in which individual POM molecules are adsorbed onto the surfaces of SWNTs without chemical decomposition. The charging/discharging measurements for the MCBs in which the cathode includes the POM/SWNT hybrid material indicate a higher battery capacity and faster charging/discharging compared with those of the microcrystalline POM MCBs. It is concluded that nanohybridization of molecular clusters with SWNTs is a promising method for improving smooth electron transport and lithium ion dispersion in battery reactions.

Received: November 18, 2010

Revised: January 10, 2011

Published online: March 8, 2011

**Keywords:** carbon nanotubes · electron transport · nanohybridization · polyoxometalates · rechargeable batteries

- [1] a) T. W. Ebbesen, H. J. Lezec, H. Hiura, J. W. Bennett, H. F. Ghaemi, T. Thio, *Nature* **1996**, 382, 54–56; b) S. J. Tans, M. H. Devoret, H. Dai, A. Thess, R. E. Smalley, L. J. Geerligs, C. Dekker, *Nature* **1997**, 386, 474–477; c) E. W. Wong, P. E. Sheehan, C. M. Lieber, *Science* **1997**, 277, 1971–1975; d) D. H. Robertson, D. W. Brenner, J. W. Mintmire, *Phys. Rev. B* **1992**, 45, 12592–12595; e) M. Ouyang, J. L. Huang, C. M. Lieber, *Acc. Chem. Res.* **2002**, 35, 1018–1025; f) P. Avouris, *Acc. Chem. Res.* **2002**, 35, 1026–1034.
- [2] T. Rueckes, K. Kim, E. Josleevich, G. Y. Tseng, C. L. Cheung, C. M. Lieber, *Science* **2000**, 289, 94–97.
- [3] a) Q. Cao, J. A. Rogers, *Adv. Mater.* **2009**, 21, 29–53; b) C. Hierold, A. Jungen, C. Stampfer, T. Helbling, *Sens. Actuators A* **2007**, 136, 51–61.
- [4] D. Vairavapandian, P. Vichchulada, M. D. Lay, *Anal. Chim. Acta* **2008**, 626, 119–129.
- [5] S. Polizu, O. Savadogo, P. Poulin, L. Yahia, *J. Nanosci. Nanotechnol.* **2006**, 6, 1883–1904.
- [6] a) Y. S. Hu, X. Liu, J. O. Muller, R. Schlögl, J. Maier, D. S. Su, *Angew. Chem.* **2009**, 121, 216–220; *Angew. Chem. Int. Ed.* **2009**, 48, 210–214; b) S. W. Lee, N. Yabuuchi, B. M. Gallant, S. Chen, B. S. Kim, P. T. Hammond, Y. S. Horn, *Nat. Nanotechnol.* **2010**, 5, 531–537; c) Y. J. Lee, H. Yi, W.-J. Kim, K. Kang, D. S. Yun, M. S. Strano, G. Ceder, A. M. Belcher, *Science* **2009**, 324, 1051–1055.
- [7] a) D. Futaba, K. Hata, T. Yamada, T. Hiraoka, Y. Hayamizu, Y. Kakudate, O. Tanaike, H. Hatori, M. Yumura, S. Iijima, *Nat. Mater.* **2006**, 5, 987–994; b) E. S. Snow, F. K. Perkins, E. J. Houser, S. C. Badescu, T. L. Reinecke, *Science* **2005**, 307, 1942–1945.
- [8] H. Yoshikawa, C. Kazama, K. Awaga, M. Satoh, J. Wada, *Chem. Commun.* **2007**, 3169–3170.

- [9] a) N. E. Chakov, M. Soler, W. Wernsdorfer, K. A. Abboud, G. Christou, *Inorg. Chem.* **2005**, *44*, 5304–5321; b) H. J. Eppley, H.-L. Tsai, N. D. Vries, K. Folting, G. Christou, D. N. Hendrickson, *J. Am. Chem. Soc.* **1995**, *117*, 301–317; c) M. Soler, P. Artus, K. Folting, J. C. Huffman, D. N. Hendrickson, G. Christou, *Inorg. Chem.* **2001**, *40*, 4902–4912; d) S. M. J. Aubin, Z. Sun, L. Pardi, J. Krzystek, K. Folting, L. C. Brunel, A. L. Rheingold, G. Christou, D. N. Hendrickson, *Inorg. Chem.* **1999**, *38*, 5329–5340; e) H. K. Bolink, L. Cappelli, E. Coronado, I. Recalde, *Adv. Mater.* **2006**, *18*, 920–923.
- [10] R. Sessoli, H.-L. Tsai, A. R. Schake, S. Wang, J. B. Vincent, K. Folting, D. Gatteschi, G. Christou, D. N. Hendrickson, *J. Am. Chem. Soc.* **1993**, *115*, 1804–1816.
- [11] a) H. Yoshikawa, S. Hamanaka, Y. Miyoshi, Y. Kondo, S. Shigematsu, N. Akutagawa, M. Sato, T. Yokoyama, K. Awaga, *Inorg. Chem.* **2009**, *48*, 9057–9059; b) H. Wang, S. Hamanaka, T. Yokoyama, H. Yoshikawa, K. Awaga, *Chem. Asian. J.* **2011**, DOI: 10.1002/asia.201000782.
- [12] a) D.-L. Long, R. Tsunashima, L. Cronin, *Angew. Chem.* **2010**, *122*, 1780–1803; *Angew. Chem. Int. Ed.* **2010**, *49*, 1736–1758; b) D.-L. Long, E. Burkholder, L. Cronin, *Chem. Soc. Rev.* **2007**, *36*, 105–121; c) C. L. Hill, *Chem. Rev.* **1998**, *98*, 1–2; d) K. Binnemans, *Chem. Rev.* **2009**, *109*, 4283–4374; e) M. T. Pope, A. Muller, *Angew. Chem.* **1991**, *103*, 56–70; *Angew. Chem. Int. Ed. Engl.* **1991**, *30*, 34–48; f) I. V. Kozhevnikov, *Chem. Rev.* **1998**, *98*, 171–198; g) J.-D. Compain, P. Mialane, A. Dolbecq, I. Martyr, Mbomekalle, J. Marrot, F. Secheresse, E. Riviere, G. Rogez, W. Wernsdorfer, *Angew. Chem.* **2009**, *121*, 3123–3127; *Angew. Chem. Int. Ed.* **2009**, *48*, 3077–3081.
- [13] a) M. Lira-Cantú, P. G. Romero, *Chem. Mater.* **1998**, *10*, 698–704; b) B. M. Azumi, T. Ishihara, H. Nishiguchi, Y. Takita, *Electrochemistry* **2002**, *70*, 869–874.
- [14] a) A. Giusti, G. Charron, S. Mazarat, J.-D. Compain, P. Mialane, A. Dolbecq, E. Riviere, W. Wernsdorfer, R. N. Biboum, B. Keita, L. Nadjjo, A. Filoramo, J.-P. Bourgoin, T. Mallah, *Angew. Chem.* **2009**, *121*, 5049–5052; *Angew. Chem. Int. Ed.* **2009**, *48*, 4949–4952; b) G. Charron, A. Giusti, S. Mazarat, P. Mialane, A. Gloter, F. Miserque, B. Keita, L. Nadjjo, A. Filoramo, E. Riviere, W. Wernsdorfer, V. Huc, J.-P. Bourgoin, T. Mallah, *Nanoscale* **2010**, *2*, 139–144.
- [15] Y. Song, E. Wang, Z. Kang, Y. Lan, C. Tian, *Mater. Res. Bull.* **2007**, *42*, 1485–1491.
- [16] C. Sanchez, J. Livage, J. P. Launay, M. Fournier, Y. Jeannin, *J. Am. Chem. Soc.* **1982**, *104*, 3194–3202.
- [17] N. Nakashima, Y. Tomonari, H. Murakami, *Chem. Lett.* **2002**, 638–639.
- [18] a) I. Imaz, F. Luis, C. Carbonera, D. R. Molina, D. Maspoch, *Chem. Commun.* **2008**, 1202–1204; b) C. Carbonera, I. Imaz, D. Maspoch, D. Ruiz-Molina, F. Luis, *Inorg. Chim. Acta* **2008**, *361*, 3951–3956.